© 2014. Published by The Company of Biologists Ltd | The Journal of Experimental Biology (2014) 217, 432-443 doi:10.1242/jeb.087569

RESEARCH ARTICLE

Compensations for increased rotational inertia during human cutting turns

Mu Qiao[1], Brian Brown[1] and Devin L. Jindrich[2,*]

ABSTRACT

Locomotion in a complex environment is often not steady state, but unsteady locomotion (stability and maneuverability) is not well understood. We investigated the strategies used by humans to perform sidestep cutting turns when running. Previous studies have argued that because humans have small yaw rotational moments of inertia relative to body mass, deceleratory forces in the initial velocity direction that occur during the turning step, or 'braking' forces, could function to prevent body over-rotation during turns. We tested this hypothesis by increasing body rotational inertia and testing whether braking forces during stance decreased. We recorded ground reaction force and body kinematics from seven participants performing 45 deg sidestep cutting turns and straight running at five levels of body rotational inertia, with increases up to fourfold. Contrary to our prediction, braking forces remained consistent at different rotational inertias, facilitated by anticipatory changes to body rotational speed. Increasing inertia revealed that the opposing effects of several turning parameters, including rotation due to symmetrical anterior–posterior forces, result in a system that can compensate for fourfold changes in rotational inertia with less than 50% changes to rotational velocity. These results suggest that in submaximal effort turning, legged systems may be robust to changes in morphological parameters, and that compensations can involve relatively minor adjustments between steps to change initial stance conditions.

KEY WORDS: Locomotion, Stability, Maneuverability, Unsteady, Sidestep, Motor control

INTRODUCTION

Maneuverability is necessary for locomotion in natural environments (Jindrich and Qiao, 2009). Maneuvers involve behaviourally generated changes to speed, direction and/or body orientation. Animals must maneuver to forage, negotiate uneven terrain or escape predation, with direct impacts on fitness (Demes et al., 1999; Dunbar, 1988; Howland, 1974; Losos and Irschick, 1996). Performance depends on morphology, behavior and motor control (Aerts et al., 2003; Alexander, 2002; Carrier et al., 2001; Dial et al., 2008; Eilam, 1994; Jindrich et al., 2006; Jindrich and Full, 1999; Jindrich et al., 2007; Van Damme and van Dooren, 1999). For humans, turns alone comprise up to 50% of walking steps during daily living (Glaister et al., 2007), and can cause injuries directly by increasing the forces and moments experienced by the legs, and indirectly by decreasing stability and causing falls (Besier et al., 2001; Colby et al., 2000; Cross et al., 1989; Kawamoto et al., 2002; McLean et al., 2004; Stacoff et al., 1996). Maneuvering performance reflects dynamic interactions among mechanics, musculoskeletal physiology and motor control (Biewener and Daley, 2007; Dickinson et al., 2000; Full et al., 2002; Jindrich and Qiao, 2009). Determining the principles governing unsteady locomotion therefore requires assessing both the mechanical requirements and behavioral compensations associated with maneuvers.

Two common aspects of maneuvers are changing movement direction and body re-orientation. Changing movement direction requires a force impulse with a component orthogonal to the initial movement direction (imd). Body re-orientation does not require external moments if large limb motions are used (Kane and Scher, 1970). However, moments due to external forces will also cause rotation if resultant forces are not directed through the center of mass (COM). For example, a simple mathematical model based on the assumptions that (1) rotational moments are primarily due to external forces and (2) body rotation should align with velocity direction at the end of a turning step can predict horizontal-plane ground reaction forces (GRFs) used during maneuvers in insects, ostriches and humans (Jindrich and Qiao, 2009). The model relates several morphological (i.e. body mass, M; yaw moment of inertia, I_{zz}), task (i.e. velocity direction change, θ_d; amount of body rotation, θ_r; and speed, $V_{AEP,imd}$) and behavioral (i.e. fore–aft foot placement, $P_{AEP,imd}$; lateral foot placement, P_p; and stance duration, τ) parameters (Fig. 1A). The model was used to express the hypothesis that braking forces, i.e. deceleratory forces in the initial velocity direction that occur during the turning step, act to control body rotation during running turns (Jindrich et al., 2006). Specifically, the model suggests that braking forces prevent body over-rotation in humans, in part because of an orthograde posture and a high ratio of M to I_{zz}. This hypothesis was supported by the 7- to 20-fold increases in braking forces during turns relative to constant-average-velocity running, the approximate doubling of average braking forces with an increase in turn magnitude from 28 to 42 deg, and the high (r^2=0.7) correlation between measured and model-predicted peak braking forces for both sidestep and crossover cuts (Jindrich et al., 2006).

Additional support was provided by the model's prediction that braking forces for ostriches, ancestrally cursorial runners with a pronograde posture and a lower ratio of M to I_{zz} relative to humans, may not be necessary to prevent over-rotation (Jindrich et al., 2007). As predicted by the model, ostriches made sidestep cuts using braking forces that were, on average, close to zero. Although the lower M to I_{zz} ratio could explain some of the low braking forces observed in ostriches, differences in several other parameters also contributed (Jindrich and Qiao, 2009). Although measured peak braking forces were tightly correlated to predictions (r^2=0.7), forces also showed substantial variance across trials, suggesting that braking forces may still contribute to trial-by-trial control of body rotation.

In addition to braking forces, other behavioral parameters could also contribute to successfully matching changes in body orientation

---

[1]Kinesiology Program, School of Nutrition and Health Promotion, Arizona State University, Phoenix, AZ 85004-0698, USA. [2]Department of Kinesiology, California State University, San Marcos, CA 92096, USA.

*Author for correspondence (djindrich@csusm.edu)

Received 28 February 2013; Accepted 30 September 2013

List of symbols and abbreviations

AEP	anterior extreme position
AP	anterior–posterior
COM	center of mass
COP	center of pressure
F'_{hmax}	predicted braking force from Eqn 3
F_{hmax}	predicted braking force from Eqn 5
$F_{\mathrm{imd}}(t)$	projection of GRF to the anterior of the initial movement direction, $V_{\mathrm{AEP,imd}}$
$F_{\mathrm{p}}(t)$	projection of GRF perpendicular to the direction of $V_{\mathrm{AEP,imd}}$, and toward a turning direction to the left
F_{pmax}	peak ML GRF, $F_{\mathrm{p}}(t)=F_{\mathrm{pmax}}\sin(\pi\ t/\tau)$
GRF	ground reaction force
imd	initial movement direction
I_{zz}	body rotational inertia
LE	updated ‘leg effectiveness number’
LGT	left greater trochanter
M	body mass
M0%I1	control, non-harness
M15%I3	mass increased by 15% and body inertia to threefold
M15%I3.5	mass increased by 15% and body inertia to 3.5-fold
M17%I3.5	mass increased by 17% and body inertia to 3.5-fold
M17%I4	mass increased by 17% and body inertia to fourfold
ML	mediolateral
NH	non-harness
$P_{\mathrm{AEP,imd}}$	AP foot placement relative to the COM at TD
P_{p}	ML foot placement relative to the COM at TD
RGT	right greater trochanter
t	time
TD	touch-down
TO	take-off
$T_z(t)$	free moment
$V_{\mathrm{AEP,imd}}$	horizontal COM velocity at TD
V_{f}	horizontal COM velocity at TO
α	magnitude of the full-sine component of $F_{\mathrm{imd}}(t)=\alpha\sin(2\pi\ t/\tau)+\beta(\pi\ t/\tau)$
β	measured peak braking force, the magnitude of the half-sine component of $F_{\mathrm{imd}}(t)$
ε	leg effectiveness number
η	correction term to account for the effects of initial and final rotation conditions
θ_{d}	COM velocity deflection angle
θ_{f}	mismatch between body orientation and COM speed at TO
θ_{Fp}	rotational angle caused by ML GRF $F_{\mathrm{p}}(t)$
θ_{i}	initial angular difference between COM velocity and body orientation
θ_{r}	body rotation angle
θ_{Tz}	rotational angle caused by free moment
θ_{α}	body rotation angle caused by $\alpha\sin(2\pi\ t/\tau)$ in $F_{\mathrm{imd}}(t)$
$\theta_{\alpha\mathrm{Fp}}$	body rotation angle caused by the interaction between α and $F_{\mathrm{p}}(t)$
θ_{β}	rotational angle balanced by braking force
τ	stance duration
ω_0	initial body rotational angular speed

to changes in velocity direction during running turns. For humans, turns of increasing magnitude were associated with increases in stance duration (τ) and foot placement in the anterior–posterior ($P_{\mathrm{AEP,imd}}$) and mediolateral (P_{p}) directions. However, these changes were not as closely associated with turn magnitude as were braking forces (Jindrich et al., 2006). Moreover, several parameters that could affect turning were not included in the analysis or model. For example, body rotation could be directly affected by initial pre-rotation angle (θ_{i}) and initial body rotational speed (ω_0; Fig. 1A). Rotation due to free moments (θ_{Tz}), i.e. rotation due to moments directly generated by the foot in contact with the ground, were small during normal running turns, but could potentially be recruited under different or perturbed turning conditions. Consequently, whether adjustments to one, or some combination, of these parameters are used to control body rotation during running turns remains a question.

One difference among parameters that could affect their role is the point in the stride cycle at which each parameter can be altered. Changes to braking force, free moment or stance duration involve alterations to forces or moments generated by the leg during stance. Changes to other parameters (e.g. $P_{\mathrm{AEP,imd}}$, P_{p}, θ_{i} or ω_0) involve altering leg or body kinematics during previous steps or the flight period before stance. Anticipation can involve adjustments to muscle activity associated with changes in foot placement and GRFs (Bencke et al., 2000; Houck, 2003; Rand and Ohtsuki, 2000). However, passive factors such as coupling among parameters (i.e. foot placement and GRFs) could also contribute to changes prior to turning steps. For simplicity, we will term ‘anticipatory’ any parameters that are determined before the turning step, whether passive (mechanical) or active factors primarily cause a change. Furthermore, observed anticipatory changes may not necessarily be involved in the trial-level control of individual turns, but could instead reflect task-level adjustments associated with the shift from constant-average-velocity running to turning (Besier et al., 2003). Consequently, the role of anticipatory adjustments relative to changes that occur during the stance period of a turning step remains unclear.

Our overall goal is to better characterize the behavioral strategies used by legged animals to perform turning maneuvers, to identify the parameters used to turn and determine how and when they are modulated to make successful turning maneuvers despite variability and perturbations. Specifically, we sought to test the hypothesis that human runners use braking forces alone to maintain appropriate body rotation during running turns under different mechanical conditions that affect body rotation. This hypothesis would be supported if perturbations that affect body rotation result in proportional changes to braking forces during stance, but do not affect other behavioral parameters. If braking forces do not change then the hypothesis is rejected, and this presents the question of whether anticipatory adjustments, within-step changes or a combination are used to compensate for perturbations to rotation.

To test this hypothesis, we sought to perturb body rotation requirements while minimally changing other aspects of turning (i.e. requirements for movement direction or linear momentum change). To this end, we used a harness system that enabled up to 400% increases in rotational inertia with substantially less (15–17%) change to body mass. If the magnitude of braking forces alone is adjusted to control body rotation, the turning model predicts that increases in I_{zz} would progressively decrease peak braking forces and even result in acceleratory forces. Threefold increases in I_{zz} would decrease peak braking forces to zero and, similar to ostriches, humans would turn using primarily the average lateral forces necessary for movement deflection.

RESULTS

Turning performance was similar among inertia conditions

Increasing rotational inertia did not change most aspects of turning performance. On average, participants made sidestep cuts with COM deflection angles (θ_{d}) and body rotational angles (θ_{r}) that were not significantly different among conditions (Table 1). However, participants did not fully deflect their movement direction by 45 deg during the turning step, but by only 25–27 deg (Table 1). This was primarily because of partially changing movement direction (relative to global) before the primary turning step. Forces in both the ML and AP directions [$F_{\mathrm{p}}(t)$ and $F_{\mathrm{imd}}(t)$, respectively] were also not significantly different (Fig. 2AB). There was no significant difference between COM initial speed ($V_{\mathrm{AEP,imd}}$) and final speed (V_{f})

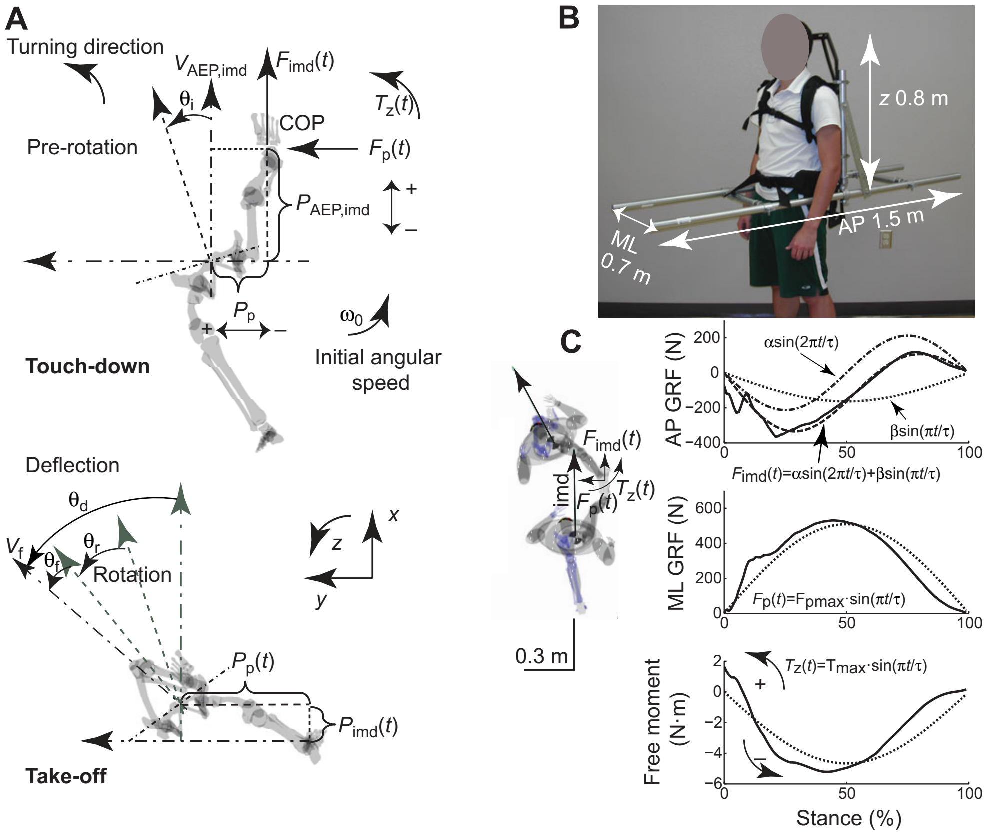

Fig. 1. Horizontal-plane turning model. (A) Body orientation at touch-down (TD; upper) and take-off (TO; lower) during sidestep cutting turns. Coordinates are relative to the initial center of mass (COM) velocity at TD ($V_{\mathrm{AEP,imd}}$). During stance, the body rotates by θ_r while the COM deflects by θ_d. At TD, there is pre-rotation between body orientation and COM velocity (θ_i). Positive θ_i indicates that body rotation precedes COM velocity direction, while negative θ_i indicates lag, and the case where $\theta_d=\theta_i+\theta_r+\theta_f$ is pictured. (B) Harness used to change body rotational inertia (I_{zz}). (C) Horizontal-plane human turning model with body posture at TD and TO. Anterior–posterior (AP) force, $F_{\mathrm{imd}}(t)$, is approximated by the combination of a full-sine wave (alpha component) and a half-sine wave (beta component, most commonly a braking force). Mediolateral (ML) force, $F_p(t)$, is approximated by another half-sine wave with peak F_{pmax}. Free moment, $T_z(t)$, is fitted by a half-sine wave with peak $T_{\max}$. In the current figure, $T_z(t)$ is negative and against turning direction. The body posture in C was first averaged across all trials within M0%I1 (control, non-harness), and then averaged across all rotational inertia levels and participants. See List of symbols and abbreviations for other definitions.

(P=0.99; Table 1). Increased force impulses associated with 15–17% increases in mass were achieved by 10–16% increases in stance duration (τ; Table 1). Consequently, because participants were able to achieve similar performance in all conditions, turns with and without the harness and under different M and I_{zz} conditions were considered comparable.

Increasing inertia did not decrease peak braking forces

Leg effectiveness number (ε) decreased significantly as rotational inertia increased (P<0.01; Table 1). Measured decreases in ε caused the predicted peak braking force, F_{hmax}, to decrease significantly and to predict acceleratory forces at M17%I3.5 and M17%I4 (P<0.01; Fig. 3A, Table 1).

However, measured peak braking force, β, was not significantly different among rotational inertia conditions (P=0.08; Table 1). Moreover, GRF impulse in the AP direction was also not different (P=0.21; Fig. 3B). Consequently, the hypothesis that increasing rotational inertia would decrease measured peak braking force was rejected.

Force direction relative to the leg did not change with increased inertia

The consistent braking forces across M and I_{zz} conditions resulted in unchanged leg orientation with respect to GRF (1.5 deg) during stance. The GRF direction relative to the virtual leg connecting the COM and the center of pressure (COP) at 50% of stance phase was unchanged during sidestep cutting turns with different I_{zz} (P=0.19; Fig. 4A). Relative angles during straight running under different I_{zz} also remained the same (P=0.48; Fig. 4B). A factorial repeated-measures ANOVA comparing the effects of gait (factor A, TURN and RUN) and I_{zz} (factor B) on body orientation relative to GRF revealed no main effects (p_A=0.9, p_B=0.2; Fig. 4C).

Both anticipatory and within-step parameters changed with increased inertia

Increased I_{zz} was associated with both changes to parameters describing the turning step and anticipatory adjustments. Significant increases in stance duration occurred during the turning step (τ, P<0.01; Table 1). ML foot placement (P_p), which reflects changes that primarily occur before the turning step, decreased 8–15% relative to non-harness (NH; M0%I1) turning. However, AP foot placement ($P_{\mathrm{AEP,imd}}$) did not differ significantly among conditions (P=0.15; Table 1). Changes to P_p were partially due to shifts of the COP under the foot. When either $P_{\mathrm{AEP,imd}}$ and P_p were determined from the toe or heel markers, there was no significant difference among inertia conditions ($P_{\mathrm{AEP,imd}}$, P=0.13; P_p, P=0.32).

All other parameters being equal, decreases in P_p would be expected to require increased peak braking force (β) (see Eqn 5 in

Table 1. Values for turning parameters for different rotational inertia TURN tasks

Parameter	Symbol (units)	P	M0%I1$^{\mathrm{I}}$	M15%I3$^{\mathrm{II}}$	M15%I3.5$^{\mathrm{III}}$	M17%I3.5$^{\mathrm{IV}}$	M17%I4$^{\mathrm{V}}$
TD speed	$V_{\mathrm{AEP,imd}}$ (m s^{-1})	0.32	2.9±0.2	2.7±0.2	2.8±0.2	2.8±0.3	2.7±0.2
TO speed	V_{f} (m s^{-1})	0.67	2.9±0.3	2.7±0.2	2.7±0.2	2.8±0.2	2.8±0.2
COM velocity deflection	θ_{d} (deg)	0.50	27±4	25±6	25±3	25±4	25±5
Body rotation	θ_{r} (deg)	0.98	13±7	13±6	13±3	12±3	12±3
Leg effectiveness number	ε	<0.01	$3.1\pm0.8^{\mathrm{II,III,IV,V}}$	1.4±1.2	$1.0\pm0.3^{\mathrm{V}}$	0.8±0.6	0.6±0.4
Predicted peak braking force	F_{hmax} (N)	<0.01	$-140\pm41^{\mathrm{III,IV,V}}$	−27±95	$-1.9\pm51^{\mathrm{V}}$	31±100	74±72
Measured peak braking force	β (N)	0.08	−130±36	−88±88	−100±37	−77±84	−68±99
AP foot placement	$P_{\mathrm{AEP,imd}}$ (m)	0.15	−0.422±0.025	−0.418±0.069	−0.434±0.024	−0.404±0.062	−0.386±0.057
ML foot placement	P_{p} (m)	<0.05	$0.248\pm0.024^{\mathrm{II}}$	0.211±0.017	0.224±0.015	0.229±0.031	0.220±0.026
Initial angular rotation speed	ω_0 (deg s^{-1})	<0.05	65±37	33±11	40±6.7	43±10	38±8.7
Stance duration	τ (s)	<0.01	$0.275\pm0.026^{\mathrm{II}}$	0.320±0.023	0.310±0.018	0.303±0.026	0.310±0.025
Angle caused by ω_0	$\omega_0\tau$ (deg)	0.17	18±10	11±3	12±2	13±4	12±3
Initial pre-rotation	θ_{i} (deg)	0.36	8±9	3±5	4±5	6±6	3±5
Final rotation mismatch	θ_{f} (deg)	0.10	4±5	10±2	8±4	6±5	10±4
Angle caused by full-sine component of $F_{\mathrm{imd}}(t)$	θ_α (deg)	<0.01	$-42\pm6^{\mathrm{III,IV,V}}$	−23±16	$-14\pm1^{\mathrm{V}}$	−14±3	−12±2
Angle caused by interaction	$\theta_{\alpha\mathrm{Fp}}$ (deg)	<0.05	$17\pm4^{\mathrm{III,IV,V}}$	11±9	7±1	6±2	6±2
Angle caused by free moment	θ_{Tz} (deg)	<0.05	$-8\pm8^{\mathrm{II}}$	1±4	0±4	−1±3	0±3

Data are means ± s.d. *P*-values are the results of the repeated measure ANOVA across those five conditions. Significant differences in *post hoc* comparisons are indicated by superscript Roman numerals ($P<0.0051$). For all angles, the positive value is along the turning direction.
AP, anterior–posterior; COM, center of mass; ML, mediolateral; TD, touch-down; TO, take-off.

Materials and methods). However, the decreases in P_{p} were more than offset by 10–16% increases in τ that would be expected both to decrease ε (see Eqn 4) and directly decrease β (see Eqn 5). Consequently, changes to the modeled parameters P_{p} and τ could not explain the unchanged peak braking forces among different rotational inertia conditions.

Changes to initial rotational velocity contributed to consistent braking forces

Increasing I_{zz} revealed that a balance among several previously unmodeled parameters resulted in unchanged β across conditions. A more complete model of turning (see Appendix) showed that perpendicular turning forces (F_{p}) and braking forces were not the only contributors to body rotation. Both the normally observed deceleratory/acceleratory AP force (the α component of F_{imd}) and its interaction with F_{p} resulted in substantial body rotations (θ_α and $\theta_{\alpha\mathrm{Fp}}$, respectively; Table 1). For example, in the NH condition these force components together resulted in net body rotations of −25 deg, i.e. against the overall turn direction. This rotation, $\theta_\alpha+\theta_{\alpha\mathrm{Fp}}$, was almost completely offset by initial body rotational velocity (ω_0) acting over the stance period, and initial body rotation (θ_{i}) at TD, that together contributed 26 deg of body rotation towards the turning direction. Therefore, for the NH condition, the small amount (~1 deg) of net body rotation resulting from the sum of these parameters ($\theta_\alpha+\theta_{\alpha\mathrm{Fp}}+\theta_{\mathrm{i}}+\omega_0\tau$) did not substantially affect the ability of the simple model of Eqns 4 and 5 to predict β with F_{hmax} (Jindrich et al., 2006).

Increasing I_{zz} significantly reduced both θ_α and $\theta_{\alpha\mathrm{Fp}}$, resulting in a combined effect of −6 to −7 deg of rotation against the turn direction for threefold and greater increases in I_{zz}. Without $\theta_\alpha+\theta_{\alpha\mathrm{Fp}}$ opposing ω_0 and θ_{i}, the potential for body over-rotation would be expected to increase. Preventing over-rotation during the turning step could be achieved by increasing peak braking forces relative to the NH condition (the opposite of the hypothesis from the simple turning model) to maintain θ_{r} close to θ_{d}. Instead, participants employed an anticipatory strategy, significantly decreasing ω_0 ($P<0.05$; Table 1). However, ω_0 did not drop to zero but decreased only by 33–49%. Therefore, rotation due to ω_0 and θ_{i} balanced rotation due to fore–aft forces, allowing for anticipatory adjustments to initial rotation conditions to maintain nearly constant braking forces among conditions.

DISCUSSION

Contrary to the hypothesis that increasing I_{zz} would decrease braking force, we found that anticipatory changes to initial rotational speed were associated with maintaining average braking forces that did not differ among rotational inertia conditions during running turns. Consistent turning performance was maintained across fourfold increases in I_{zz} using relatively minor changes to behavioral parameters: 8–15% decreases in ML foot placement (P_{p}), 10–16% increases in stance duration (τ) and 33~49% decreases in initial rotational angular speed (ω_0). Moreover, the opposing rotation of multiple dynamic parameters provided humans with several behavioral options when compensating for morphological changes.

Peak braking forces did not decrease as much as predicted, maintaining consistent force direction relative to the leg

Based on the turning model and the relatively small braking forces observed in ostriches, we predicted that humans would decrease peak braking forces when the requirements for preventing body over-rotation were relaxed. Humans instead maintained similar peak braking forces and GRF orientation relative to the leg across fourfold changes to rotational inertia. There was a trend for decreases in β with increased inertia that may have been non-significant because of limited sample size. However, the ~50% decreases in measured β would have been insufficient to explain the 150% decreases in F_{hmax} predicted to control body rotation with braking forces alone. The maintenance of similar leg forces across conditions may limit the changes in motor output required for different maneuvers. Similar to ostriches, where cutting turns involved few changes to joint moments relative to straight running (Jindrich et al., 2007), humans may organize maneuvers in part to reduce functional changes at the joint or muscle level.

Several task objectives may influence the strategies used to perform maneuvers

Our simplified model relates morphological, task and behavioral parameters based on the assumption that the body should rotate appropriately in the movement direction. However, maneuvers may also be organized to achieve other objectives. For example, braking forces contribute to turn sharpness (Houck, 2003). Braking forces could also act to maintain consistent average speed after the turning

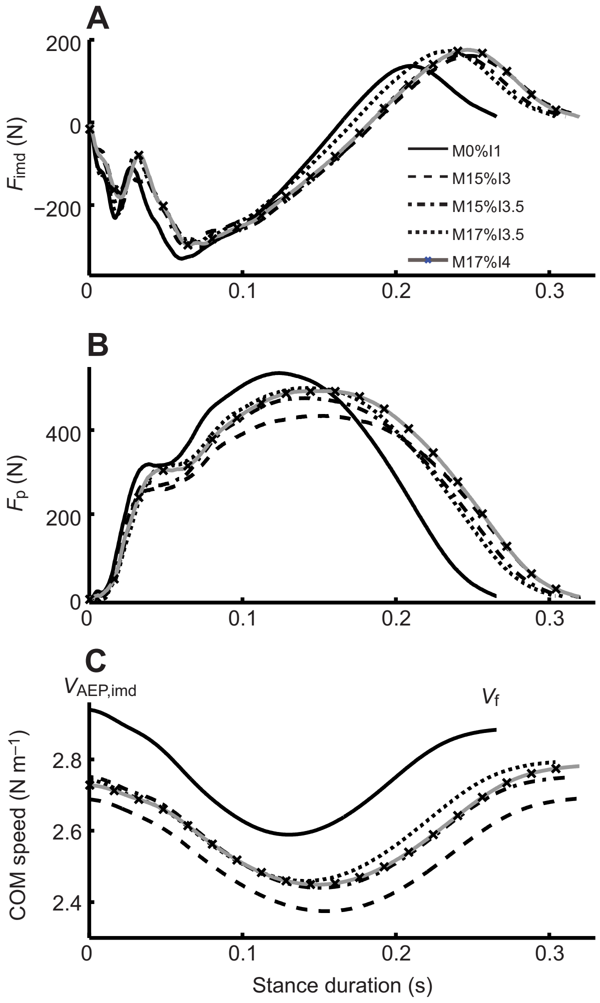

Fig. 2. Force and COM speed profile ensembles for different rotational inertias for the stance phase of the turning step. (A) F_{imd} and (B) F_{p} are the GRF projections along and perpendicular to initial COM velocity at TD ($V_{\mathrm{AEP,imd}}$). (C) COM speed in the horizontal plane first decreased and then increased back to the original value. Different rotational inertias are represented by different line types; M0%, M15% and M17% indicate the percentage of mass increase, and I1, I2, I3.5 and I4 indicate the fold increase in body rotational inertia. Each line is the ensemble average of all trials within the same rotational inertia for the same participant, and then averaged across participants.

step by offsetting the acceleration from the F_{p} necessary to change movement direction. In support of this possibility, there was no significant difference between COM speed at TD ($V_{\mathrm{AEP,imd}}$) and at TO (V_{f}) (P=0.99; Fig. 2C). For individual trials, speed at TO was correlated with speed at TD (R^2=0.55; Fig. 5A). The braking forces necessary for speed at TO to equal speed at TD can be predicted for a simple point-mass model as:

$$\frac{M\pi}{2\tau}V_{\mathrm{AEP,imd}}\left(\cos\theta_{\mathrm{d}}-1\right). \tag{1}$$

Braking forces required for constant speed were correlated with measured forces (slope=0.3 and R^2=0.43; Fig. 5B). We therefore cannot reject the hypothesis that constant-speed movement is an objective. However, measured braking forces were larger than forces predicted by the point-mass model (resulting in a slope <1).

Therefore, although movement parameters are related in a way that results in appropriate body rotation and can be predicted by Eqns 2 and 3, we cannot conclude that these relationships reflect active control of body orientation. Additional experiments will be necessary to determine how movement is organized to satisfy several task objectives of potentially different importance, including controlling body rotation, maintaining speed, maximizing stability, reducing injury risk, minimizing energetic cost, or reducing sensorimotor demands.

Whether the strategies used by bipeds for maneuvers are also employed by other animals also remains an important question. Quadrupeds or polypeds that step with more than one leg may have fewer constraints and more options for maneuvering strategies than bipeds (Jindrich and Full, 1999). For example, additional legs may allow for rotation and translation to become partially de-coupled (Walter, 2003).

Anticipatory changes contributed to consistent peak braking forces

Anticipatory adjustments contributed to appropriate body rotation. Increasing I_{zz} resulted in significant differences in anticipatory (ML foot placement, P_{p}, and initial angular speed, ω_0) parameters and to parameters describing the turning step (stance duration, τ). However, observed increases in τ could be primarily due to increases in body mass (M) resulting from the harness and weights. Although our original intent for using two separate levels of added mass was to directly test the effects of M on turning, constraints on the length of the harness bars limited our values of M to differing by only 2%. Longer galvanized steel bars substantially increased M and offset the benefit of requiring less added weight to increase I_{zz}. However, as M and I_{zz} increased, τ increased by 15–20% even in the RUN condition (P<0.05; Table 2). Similarly, increasing M alone by 10% or 20% was found to result in 5% or 8% increases in τ during constant-speed treadmill running at 3 m s^{-1} (Chang et al., 2000). Therefore, it is reasonable to conclude that the increases in τ are associated with increased M and not I_{zz}.

If increases in stance duration reflected compensations for increased mass, compensations for increased I_{zz} principally involved significant changes in two parameters that were both primarily determined before the turning step: ML foot placement (P_{p}) and initial body rotational speed (ω_0). For all turning conditions, humans increased their lateral leg placement relative to straight running (RUN), where P_{p} averages ~4 cm (Jindrich et al., 2006). The higher P_{p} observed during turns compared with RUN could reduce the braking forces necessary to prevent over-rotation, and would therefore be consistent with the hypothesis that humans reduce braking forces when less necessary because of increased I_{zz}. However, increases in I_{zz} were instead associated with decreased P_{p} relative to the NH condition, consistent with the alternative hypothesis that humans use anticipatory adjustments to maintain unchanged braking forces during running turns.

In contrast to changes in ML foot placement, decreases in ω_0 with increased I_{zz} relative to the NH condition would be expected to decrease peak braking forces. However, the values of ω_0 were high in the NH condition (65 deg s^{-1}) and remained positive despite 33–49% decreases with increased I_{zz} (Table 1). Therefore, along with pre-rotation (θ_{i}), ω_0 continued to cause rotation in the trial turn direction. Overcoming rotation due to ω_0 contributed to required braking forces in all conditions. Without decreases in ω_0, peak braking forces in the increased I_{zz} conditions could even have increased relative to NH values. Therefore, the decreases in ω_0 relative to the NH condition were also consistent with the hypothesis that humans use anticipatory adjustments to maintain unchanged peak braking forces during running turns. Anticipatory adjustments that reflect behavioral

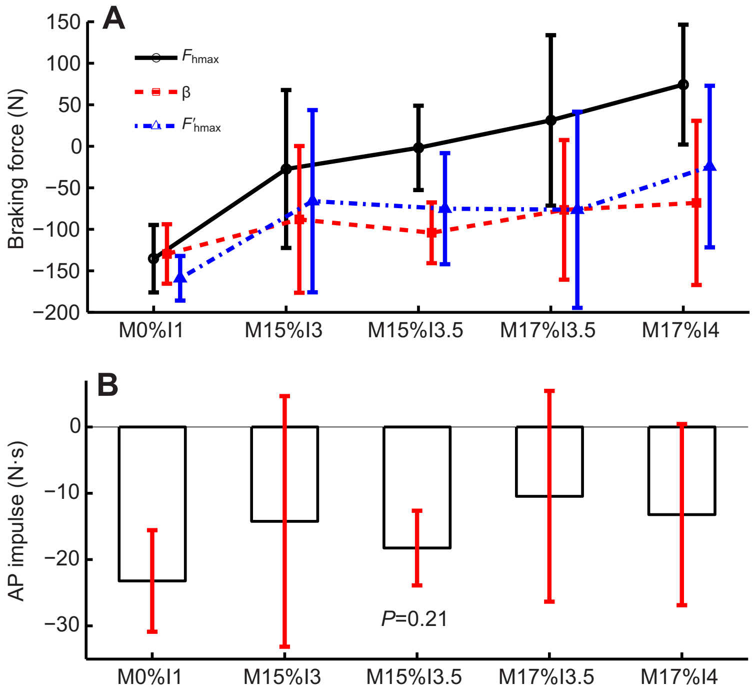

Fig. 3. Peak braking forces for different mass and rotational inertia conditions. (A) The effects of rotational inertia on average predicted and measured peak braking forces. Negative values indicate deceleration in the initial COM velocity direction ($V_{AEP,imd}$), and positive values indicate acceleration. F_{hmax} (black solid line) is the braking force predicted from the original model (Eqn 5); β (red dashed line) is the measured peak braking force; F'_{hmax} (blue dashed and dotted line) is the predicted braking force from the revised model, as expressed in Eqn 3. (B) Averaged net AP impulse for different rotational inertia conditions. Data are means ± s.d.

strategies are consistent with research on walking turns (Jindrich and Qiao, 2009). For example, anticipation in walking turns affects foot placement (Orendurff et al., 2006; Patla et al., 1999), and changes to ω_0 and θ_i are initiated before the turning step in walking (Taylor et al., 2005). The finding that anticipatory compensations are used during both walking and running could therefore suggest that humans use some feed-forward strategies to execute anticipated maneuvers.

However, because initial rotational speed reflects the dynamics of strides before the turn that could be affected by increased I_{zz}, we cannot determine whether decreases in ω_0 were due to behavioral adjustments or stemmed passively from changes in running dynamics associated with higher M and I_{zz}. Decreases in ω_0 in the RUN condition (Table 2) for increased I_{zz} suggest that the compensations necessary to maintain unchanged braking forces may arise passively, or be part of a more general strategy for compensation for increased inertia. Future experiments may be able to distinguish between robustness of the mechanical system and behavioral strategies that allow modest changes to initial conditions to compensate for large morphological perturbations.

Coupling among morphology, dynamics and behavior could affect the parameters chosen for compensation

A running, segmented system involves many morphological and behavioral factors that are extensively coupled. Coupling can

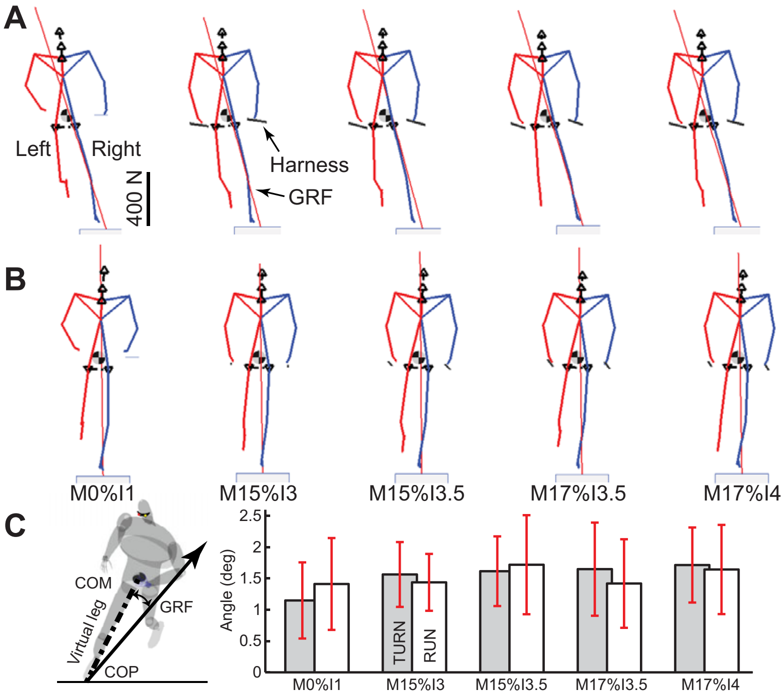

Fig. 4. Ground reaction forces relative to the body in different rotational inertia conditions. Body posture and GRF are shown at 50% of stance phase during all (A) TURN and (B) RUN tasks. (C) Definition of the angle between GRF and virtual leg connecting the COM and the center of pressure (COP) at 50% of stance. This angle was not significantly influenced by either task (p_A=0.9) or rotational inertia (p_B=0.2). Data represent means of all replicate trials within each rotational inertia conditions, in turn averaged across all participants. The COM represents the overall calculated COM position for human and harness together. The views are from the back: the participant is running into the paper with the right foot in stance.

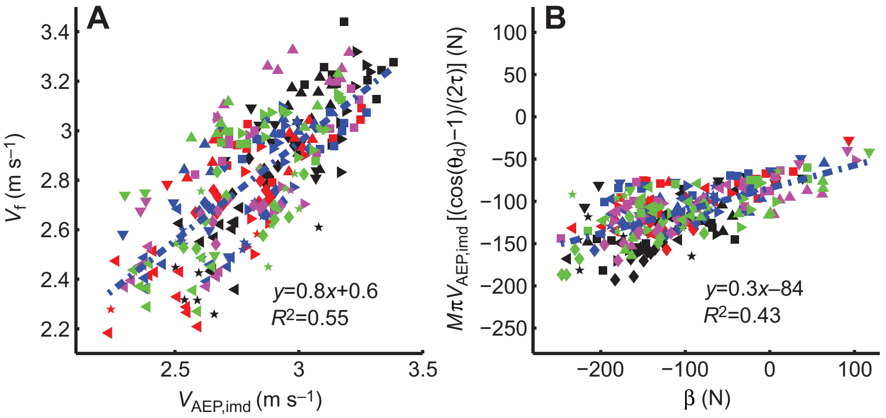

Fig. 5. Potential influence of maintaining constant speed to turning strategy. (A) Relationship between COM speed at TO (V_f) and TD ($V_{AEP,imd}$). (B) Peak braking force necessary to maintain COM speed at TO the same as at TD. Different rotational inertias are different colors: black, M0%I1; red, M15%I3; blue, M15%I3.5; magenta, M17%I3.5; and green, M17%I4. Each symbol represents an individual participant.

involve both passive mechanisms (due to changes in movement dynamics) and active coupling, where adjustments are made to achieve task requirements and mechanical or energetic objectives (Hackert et al., 2006). For example, decreased AP foot placement ($P_{AEP,imd}$) would be predicted to decrease body rotation (see Eqns 4, 5, and Eqn A10 in the Appendix). However, decreasing $P_{AEP,imd}$ could result in transfer of potential to kinetic energy, COM acceleration and increased speed (McGowan et al., 2005; Qiao and Jindrich, 2012). Changes to stance duration could alter both translational and rotational momentum changes about all three axes, potentially altering movement dynamics (Herr and Popovic, 2008).

We hypothesize that adjusting initial rotational speed is advantageous because changes to ω_0 can directly affect body rotation, depending only on stance duration (see Eqn A10). However, this presents the question of why humans did not change pre-rotation to compensate for increased I_{zz}, as θ_i can also directly change net body rotation. Changes in θ_i may not have been used because θ_i influences the orientation of the leg relative to the body at TD, potentially requiring substantial changes in muscle activity to ensure that leg forces remain appropriate, and that resultant leg forces are minimally affected by turning.

Accounting for coupling among movement parameters and initial rotation conditions allows for refinement of the simplified model

Perturbing locomotion by increasing I_{zz} demonstrated that several simplifying assumptions made in the original model (see Eqns 4, 5) were not appropriate for a general description of horizontal-plane maneuvers.

First, the model simplified COM motion in the initial movement direction by assuming constant speed. This allowed foot movement relative to the COM to be described as $P_{imd}(t)=P_{AEP,imd}-V_{AEP,imd}\cdot t$ (Jindrich et al., 2006). Accounting for accelerations during stance caused by forces in the initial movement direction (see Eqn A3 in the Appendix) resulted in two additional terms, θ_α and $\theta_{\alpha Fp}$ (Eqn A10). The net effect of $\theta_\alpha+\theta_{\alpha Fp}$ would be rotation against the turning direction, leading to predictions of lower peak braking forces.

Second, the original model neglected initial body rotation conditions, initial rotational speed (ω_0) and pre-rotation (θ_i). Both ω_0 and θ_i were positive, towards the trial turn direction, and would be expected to contribute to over-rotation and lead to a prediction of increased peak braking forces.

Third, the model also assumed that body rotation (θ_r) matched movement deflection (θ_d) at the end of the turn. However, total body rotation was less than movement deflection at TO across all conditions, suggesting that humans may prefer to consistently under-rotate during stance (Table 1, Fig. 6). Maintaining under-rotation would be predicted to require increased peak braking forces. Finally, the original model did not account for moments generated by the foot, θ_{Tz}.

Accounting for these parameters allows for a more complete description of the relationships among factors that contribute to body rotation, θ_r (see Eqn A10 in the Appendix). Using this more complete description, the leg effectiveness number can be revised to include the effects of fore–aft forces:

$$\mathrm{LE}=\frac{\theta_{Fp}+\theta_\alpha+\theta_{\alpha Fp}}{\theta_d}\,. \qquad (2)$$

Table 2. Values for turning parameters for different rotational inertia RUN tasks

Parameter	Symbol (units)	P	M0%I1$^{\text{I}}$	M15%I3$^{\text{II}}$	M15%I3.5$^{\text{III}}$	M17%I3.5$^{\text{IV}}$	M17%I4$^{\text{V}}$
TD speed	$V_{AEP,imd}$ (m s^{-1})	0.26	3.2±0.2	3.0±0.2	3.0±0.2	3.1±0.2	3.1±0.2
TO speed	V_f (m s^{-1})	<0.01	3.2±0.2	3.0±0.2	3.0±0.2	3.1±0.3	3.0±0.2
COM velocity deflection	θ_d (deg)	0.38	0±1	1±1	0±1	0±1	0±1
Body rotation	θ_r (deg)	<0.01	−10±4	−8±5	−4±4	−7±3	−4±2
Leg effectiveness number	ε	0.25	−0.3±3.0	1.6±1.3	0.5±0.9	0.6±0.8	0.4±0.9
AP foot placement	$P_{AEP,imd}$ (m)	0.06	−0.321±0.085	−0.441±0.040	−0.399±0.065	−0.407±0.074	−0.404±0.084
ML foot placement	P_p (m)	0.24	0.058±0.030	0.071±0.033	0.060±0.024	0.053±0.026	0.052±0.035
Initial angular rotation speed	ω_0 (deg s^{-1})	<0.05	−25±7	−26±18	−12±14	−27±12	−13±5
Stance duration	τ (s)	<0.05	0.248±0.022$^{\text{II,III,V}}$	0.299±0.028	0.293±0.017	0.287±0.022	0.297±0.024
Angle caused by ω_0	$\omega_0\tau$ (deg)	<0.05	−6±2	−8±6	−3±4	−8±3	−4±2
Initial pre-rotation	θ_i (deg)	0.37	3±4	4±4	0±4	0±7	1±4
Final rotation mismatch	θ_f (deg)	0.68	7±4	5±7	3±5	6±6	4±6

Data are means ± s.d. P-values are the results of the repeated measure ANOVA across the five conditions. Significant differences in *post hoc* comparisons are indicated by superscript Roman numerals (P<0.0051). For all angles, the positive value is along the turning direction.

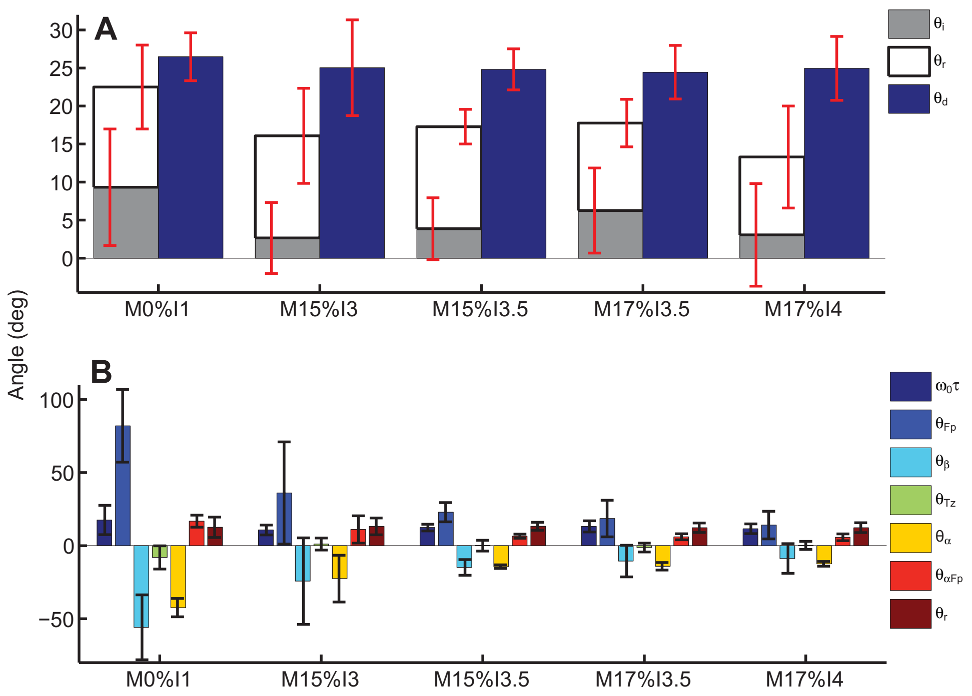

Fig. 6. Opposing contributions of different factors to body rotation during turns with different rotational inertias. (A) COM deflection (θ_d) compared with the two components of body rotation: pre-rotation (θ_i) and body rotational angle (θ_r). (B) Body rotation (θ_r) and its components caused by ML GRF (θ_{Fp}), initial body rotational angular speed ($\omega_0\tau$), braking force (θ_β), free moment (θ_{Tz}), alpha component in F_{imd} (θ_α) and the interaction between alpha component and F_p ($\theta_{\alpha Fp}$). Data are means ± s.d.

The variance in peak braking forces can then be predicted based on LE and a term representing the contribution of initial rotational conditions ($\omega_0\tau$ and θ_i) and the preference for under-rotation during the turning step (θ_f), η [which is defined as: $(\omega_0\tau+\theta_i+\theta_f)/\theta_d$]:

$$F'_{\text{hmax}} = \frac{\pi I_{zz}\theta_d}{\tau^2 P_p}\left(1-\text{LE}-\eta\right). \qquad (3)$$

Because they are consistently small during running turns (Table 1, Fig. 6B), effects of free moments (T_z) have been omitted from Eqn 3 for simplicity. However, inclusion of free moments may be necessary to describe walking or other related tasks (Lee et al., 2001; Orendurff et al., 2006). The more general relationship of Eqn 3 results in better fits to measured braking forces (Fig. 3A, Fig. 7B). For these estimates, the consistent preference for under-rotation that we observed was estimated using a constant value of 4.1 deg for θ_f. Importantly, it is necessary to include all of these additional factors in the model. Because components act to rotate the body in different directions, addition of any single factor results in fits that are poorer than those of Eqns 4 and 5 (see Materials and methods).

A balance of opposing factors could contribute to the robustness of legged maneuvers

Increased rotational inertia is often assumed to limit maximal turning performance (Carrier et al., 2001; Eilam, 1994). However, we found that increasing I_{zz} up to fourfold during sub-maximal turns did not affect performance, and could be compensated with changes to a limited number of parameters. Compensations for increased I_{zz} were facilitated by the opposite contributions of several factors to body rotation. The initial conditions (ω_0 and θ_i), and the preference for under-rotation during the turning step (θ_f), opposed the effects of rotation due to fore–aft and perpendicular forces, $\theta_\alpha+\theta_{\alpha Fp}$ (Fig. 6B, Table 1). Consequently, when increased I_{zz} decreased rotation due to

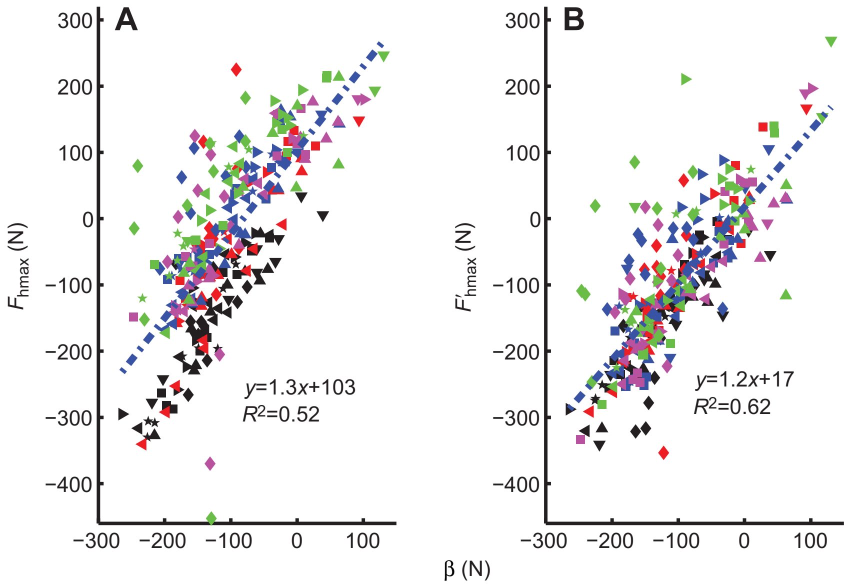

Fig. 7. Relationships between measured (β) and predicted peak braking force. (A) F_{hmax} from the original turning model as expressed by Eqn 5; (B) F'_{hmax} from Eqn 3. The definitions of symbols follow Fig. 5.

forces and their resulting moments, force directions relative to the leg could be maintained by decreased ω_0. Therefore, the opposition of rotations due to $\theta_\alpha+\theta_{\alpha Fp}$, ω_0 and θ_i contributed to the robustness of the maneuvering system by allowing substantial increases to I_{zz} to be overcome by modest changes to initial rotational speed. The robustness and stability gained from maintaining a balance of opposing factors may be analogous to the observation of increased muscle co-activation with increasing movement accuracy demands (Gribble et al., 2003).

Turning remains associated with high inter-trial variability

Humans maintained unchanged braking forces and consistent force direction relative to the leg across I_{zz} conditions by altering initial conditions, ML foot placement (P_p) and initial body rotational speed (ω_0). These findings suggest that humans are able to modulate several parameters to maintain specific aspects of movement invariant, on average. However, the ability to maintain consistent peak braking force (β) across rotational inertia conditions does not explain the large variance in many parameters, including β, across trials. For example, across-trial variability in β was 83% of the average, s.d./mean. However, the large variance observed in individual parameters contrasts with lower variance when the coupling among movement parameters described by Eqns 2 and 3 is accounted for (Fig. 7). The observation of a relationship among parameters that is maintained despite large variance in values of the parameters themselves is analogous to the pattern observed in joint coordination during several types of movements (Scholz and Schöner, 1999). For example, during hopping, joint redundancy is used to maintain task-level parameters such as leg length, orientation or force invariant (Auyang et al., 2009; Yen and Chang, 2010). Redundancy among several factors that contribute to body rotation could be exploited to maintain desired orientation relative to movement direction at the end of the turning step. However, the underlying source of the considerable intra-trial variability remains to be determined.

MATERIALS AND METHODS

All procedures used for these experiments were approved by the Institutional Review Board of Arizona State University.

Turning model

The model (Fig. 1A) assumes that an individual approaches touch-down (TD) at a horizontal speed of $V_{AEP,imd}$ (AEP, anterior extreme position; imd, initial movement direction) and makes a turn that changes COM velocity direction by the COM deflection angle, θ_d, over a stance duration of τ. Relative to the COM, the foot is placed a distance of P_p in the mediolateral (ML) direction and $P_{AEP,imd}$ in the anterior–posterior (AP) direction. The foot generates a half-sine-shaped ML force, $F_p(t)$, with a peak of F_{pmax}, and an AP force, $F_{imd}(t)$, that is the superposition of a full sine wave (with a peak of α) and half-sine acceleratory or deceleratory force (peak β; Fig. 1C) (Jindrich et al., 2006). Because the foot is initially placed anterior to the COM and moves posteriorly relative to the COM during stance, $F_p(t)$ causes a moment that initially rotates the body in the turning direction, but rotates against the turning direction after approximately mid-stance. The 'leg effectiveness number' (ε) is defined as the body rotation caused by $F_p(\tau)$, θ_{Fp}, relative to θ_d:

$$\varepsilon = \frac{\theta_{Fp}}{\theta_d} = \frac{MV_{AEP,imd}\tau}{2I_{zz}}\left(P_{AEP,imd} - \frac{4V_{AEP,imd}\tau}{\pi^2}\right). \qquad (4)$$

Peak acceleratory/deceleratory force, F_{hmax}, is the model prediction of β, and can be calculated using Eqn 5 (Jindrich et al., 2006):

$$F_{hmax} = \frac{\pi I_{zz}\left(1-\varepsilon\right)\theta_d}{\tau^2 P_p}. \qquad (5)$$

Predicted and measured deceleratory forces, F_{hmax} and β, were defined to be negative and acceleratory forces positive. Assumptions of this model include: (1) successful turns involve body rotation (θ_r) matching θ_d at the end of the turning step; and (2) initial body pre-rotation angle (θ_i) and angular speed (ω_0) are zero (Fig. 1A).

For humans, the ε during running cuts ranges from ~2 to ~4 (Jindrich et al., 2006). Consequently, during turns, the difference (1–ε) in Eqn 5 is typically negative, resulting in negative ('braking') F_{hmax}. Increasing I_{zz} would be expected to reduce ε, in turn reducing 1–ε and therefore reducing the braking forces required for θ_r to match θ_d at the end of the step.

Participants and anthropometric data

Seven participants [age=22.5±1.5 years; body mass (M)=68.2±4.0 kg; body height=174.9±4.2 cm, leg length=96.1±4.6 cm, five males; means ± s.d.] participated in the study. Anthropometric data for individual participants were estimated using allometric scaling from a reference human model, assuming identical density and segment mass percentage (Herr and Popovic, 2008; Huston and Passerello, 1982). The principal moments of inertia of each segment in yaw, roll and pitch directions were then scaled. Whole body moment of inertia tensor relative to the COM in the stance posture, as a function of M and body height, was calculated using the parallel axis theorem. This resulted in body rotational inertia, I_{zz}, scaling with $M^{5/3}$ (Carrier et al., 2001). The participant's body rotational inertia about the vertical axis was validated by having participants make stationary turns on a force platform, and calculating I_{zz} using a least-squares fit to free moment and rotation angular acceleration [validation R^2=0.72 (Jindrich et al., 2007)].

Harness

A customized harness (8.3 kg) based on previous designs was built using galvanized steel bars and a rigid plastic frame (Carrier et al., 2001). The harness was used to change I_{zz} by adding equally balanced weights (tiny lead balls contained in a bag) both anterior and posterior to the COM (Fig. 1B). The dimensions of the harness were 0.7×1.5×0.8 m (ML×AP×z). Treated as a rigid body, its principal moments and products of inertia were 1.35 (ML), 0.100 (ML, AP), 0.463 (ML, z), 0.601 (AP), 0.0972 (AP, z) and 1.38 (z) kg m^2, determined by measuring swinging periods about principal axes and the parallel axis theorem (Jindrich and Full, 1999).

Moment of inertia increase

Five different harness mass and I_{zz} increment combinations were applied: M0%I1 (control, no harness, NH), M15%I3 (mass increased by 15% and body inertia to threefold), M15%I3.5, M17%I3.5 and M17%I4. To change I_{zz}, mass was attached to the horizontal bars symmetrically about the COM of the combined human and harness. The added weight was selected so that the total weight with the harness was a set percentage (15% or 17%) of the participant's M. Both weight and position were changed to achieve the target body mass and I_{zz} increments. For example, for the M15%I3.5 condition, less weight was placed further from the COM, while for the M17%I3.5 more weight was placed closer. The specific weights and positions were calculated separately for each participant.

Experimental procedure

Participants ran at 2.98±0.08 m s^{-1}, and performed both straight running (RUN) and left 45 deg sidestep cutting turns (TURN). Turning direction was indicated by tape on the floor. In each condition, five trials were collected. The order of the conditions (RUN and all TURN conditions) was randomized. Participants were given instructions to make turns in a natural way, but were not instructed to maintain constant speed during the turn.

We used a 3-D motion tracking system (VICON, model 612, Oxford Metrics, Oxford, UK) to record the kinematics of 37 reflective markers at 120 Hz. To compensate for the harness, we replaced the markers on the anterior and posterior superior iliac spines in the standard marker set with markers on the left and right greater trochanter (LGT and RGT). Two force platforms (400×600 mm, model FP4060-NC, Bertec Corporation, Columbus, OH, USA) embedded in the ground were used to record GRF at 3000 Hz. The inertial coordinate system was defined as in Fig. 1A. The AP and ML directions were defined as parallel and perpendicular, respectively, to the horizontal projection of COM velocity at TD (i.e. the initial movement direction; Fig. 1C). Forces in the AP direction can be decomposed into full-sine (α) components similar to those observed during constant-speed running, and half-sine (β) components only observed during turning (Jindrich et al., 2006). The α and β components in $F_{\mathrm{imd}}(t)$ were determined by multiple linear regression using $\alpha\sin(2\pi\ t/\tau)$ and $\beta\sin(\pi\ t/\tau)$, respectively.

The COM was calculated by segmental average, and its velocity was tuned with the GRF using a path-finding algorithm (McGowan et al., 2005). Specifically, the initial velocity that minimized the Euclidean distance between the tuned and un-tuned COM trajectories was chosen. Body rotation (θ_r) was defined as the change in the vector connecting the hip markers (LGT and RGT; Fig. 1A) over the turning step. We also tuned rotational angle with resultant vertical moment to determine the initial rotational angular speed (ω_0) at the beginning of a turn. The correlation between tuned and un-tuned rotational angle trajectories was 0.99.

Because the harness was at the height of the pelvis, LGT and RGT markers were not visible in some of the trials. Those trials were excluded from analysis, but at least one trial for each participant at each condition was available. Only two participant/condition sets had only one trial as a result of marker placement. Eighty-three percent of the participant/condition sets contained five trials. For turning, 284 trials were successful out of 420.

Kinematic data were interpolated to the same sampling frequency as GRF using a spline fit. The instant of TD was determined as the first sample after which raw vertical GRF continuously increased for 5 ms (Qiao and Jindrich, 2012). An equivalent criterion was used to identify the last 5 ms of force decrease to identify TO. Because the COP location at TD can be noisy because of impact transients, we used the average COP location during stance relative to the toe marker to calculate $P_{\mathrm{AEP,imd}}$ and P_{p} (Jindrich et al., 2006). Kinetics/kinematics were filtered by a fourth-order zero-lag low-pass Butterworth digital filter at 30/11 Hz.

To compare the effect of rotational inertia (different M and I_{zz} combinations) on turning performance, we used repeated-measures ANOVA with participants as the repeated factor (Keppel and Wickens, 2004). To compare the effects of gait and rotational inertia on the gait parameters, a factorial repeated-measures ANOVA was employed with gait (TURN versus RUN) as factor A and the levels of different rotational inertias as factor B. *Post hoc* analysis was based on the Bonferroni procedure with Šidák correction $\{P<[1-(1-\alpha)^{1/c}]$, where $c=(a-1)\cdot a/2$ and a is the number of I_{zz} levels; this resulted in $P<0.0051\}$.

All calculations were performed using MATLAB (R2012a, MathWorks, Natick, MA, USA). All values within the text and tables are means ± s.d. except as indicated.

APPENDIX

Re-derivation of the turning model

Relaxing the assumptions of constant speed and zero rotational initial conditions requires a re-derivation of the turning model. Assuming the AP direction GRF, F_{imd}, is given by:

$$F_{\mathrm{imd}}(t)=\alpha\sin\frac{2\pi t}{\tau}+\beta\sin\frac{\pi t}{\tau}\,, \tag{A1}$$

then AP direction speed during turning is a function of time:

$$V_{\mathrm{imd}}(t)=-\frac{\tau}{\pi M}\left[\alpha\left(\cos\frac{2\pi t}{\tau}-1\right)+\beta\left(\cos\frac{\pi t}{\tau}-1\right)\right]+V_{\mathrm{AEP,imd}}\,. \tag{A2}$$

Integrating $V_{\mathrm{imd}}(t)$ with respect to time results in AP COM displacement:

$$\begin{aligned}x_{\mathrm{imd}}(t)=&-\frac{\tau^2}{\pi^2 M}\left(\frac{\alpha}{4}\sin\frac{2\pi t}{\tau}+\beta\sin\frac{\pi t}{\tau}\right)\\&+\left(V_{\mathrm{AEP,imd}}+\frac{\alpha+2\beta}{2\pi M}\tau\right)t+P_{\mathrm{AEP,imd}}\,.\end{aligned} \tag{A3}$$

The projection of the GRF along the ML direction is approximated by:

$$F_{\mathrm{p}}(t)=F_{\mathrm{pmax}}\sin\frac{\pi t}{\tau}\,. \tag{A4}$$

According to the definition, the COM velocity at TD is perpendicular to the ML direction. The COM speed along the ML direction as a function of time is therefore given by:

$$V_{\mathrm{p}}(t)=\frac{F_{\mathrm{pmax}}\tau}{\pi M}\left(1-\cos\frac{\pi t}{\tau}\right). \tag{A5}$$

Integrating with respect to time results in the COM displacement in the ML direction:

$$x_{\mathrm{p}}(t)=-\frac{F_{\mathrm{pmax}}}{M}\left(\frac{\tau}{\pi}\right)^2\sin\frac{\pi t}{\tau}+\frac{F_{\mathrm{pmax}}\tau}{\pi M}t+P_{\mathrm{p}}\,. \tag{A6}$$

Free moment is approximated by a half-sine wave in stance phase:

$$T_{\mathrm{z}}(t)=T_{\mathrm{max}}\sin\frac{\pi t}{\tau}\,. \tag{A7}$$

Hence, the net moment applying to COM in stance phase is:

$$T(t)=x_{\mathrm{p}}(t)F_{\mathrm{imd}}(t)-x_{\mathrm{imd}}(t)F_{\mathrm{p}}(t)+T_{\mathrm{z}}(t). \tag{A8}$$

Integrating with respect to time results in the angular speed in stance phase:

$$\dot{\theta}(t)=\omega_0-\frac{1}{I_{zz}}\frac{\tau}{\pi}\left\{\begin{aligned}&F_{\mathrm{pmax}}\left(V_{\mathrm{AEP,imd}}+\frac{\alpha}{2M}\frac{\tau}{\pi}\right)\left(\frac{\tau}{\pi}\sin\frac{\pi t}{\tau}-t\cos\frac{\pi t}{\tau}\right)\\&+2\left(\sin\frac{\pi t}{2\tau}\right)^2\left(-T_{\mathrm{max}}-P_{\mathrm{p}}\beta+F_{\mathrm{pmax}}P_{\mathrm{AEP,imd}}\right)\\&-P_{\mathrm{p}}\alpha\left(\sin\frac{\pi t}{\tau}\right)^2-\left\{F_{\mathrm{pmax}}\frac{\alpha}{2M}\left(\frac{\tau}{\pi}\right)^2\right.\\&\left.\left[-\left(\sin\frac{\pi t}{\tau}\right)^3+\sin\frac{\pi t}{\tau}\cos\frac{\pi t}{\tau}-t\frac{\pi}{\tau}\cos\frac{2\pi t}{\tau}\right]\right\}\end{aligned}\right\}. \tag{A9}$$

Finally, integrating $\dot{\theta}(t)$ during the stance phase results in the angular displacement by the end of turning at TO:

$$\begin{aligned}\theta_{\mathrm{r}}(\tau)&=\int_0^{\tau}\left(\int_0^{t}\frac{T(\lambda)}{I_{zz}}\mathrm{d}\lambda\right)\mathrm{d}t+\int_0^{\tau}\omega_0\mathrm{d}t\\&=-\frac{\tau^2}{\pi^3 I_{zz}}\left(4V_{\mathrm{AEP,imd}}\tau+\pi^2 P_{\mathrm{AEP,imd}}\right)F_{\mathrm{pmax}}+\frac{P_{\mathrm{p}}\beta}{I_{zz}\pi}\tau^2\\&\quad-\frac{8F_{\mathrm{pmax}}\tau^4\alpha}{3\pi^4 MI_{zz}}+\frac{P_{\mathrm{p}}\alpha}{2I_{zz}\pi}\tau^2+\frac{T_{\mathrm{max}}}{I_{zz}\pi}\tau^2+\omega_0\tau\,.\end{aligned} \tag{A10}$$

The first component of the right side of the equals sign in Eqn A10:

$$-\frac{\tau^2}{\pi^3 I_{zz}}\left(4V_{\mathrm{AEP,imd}}\tau+\pi^2 P_{\mathrm{AEP,imd}}\right)F_{\mathrm{pmax}}\,, \tag{A10.1}$$

represents rotation due to F_{p}, and can be abbreviated $\theta_{F\mathrm{p}}$. The second component:

$$\frac{P_{\mathrm{p}}\beta}{I_{zz}\pi}\tau^2\,, \tag{A10.2}$$

is the rotational angle caused by braking force along the turning direction, and can be abbreviated θ_β. The third component:

$$-\frac{8F_{\mathrm{pmax}}\tau^4\alpha}{3\pi^4 MI_{zz}}\,, \tag{A10.3}$$

is the angle caused by the interaction between the alpha component and $F_{\mathrm{p}}(t)$, and can be abbreviated $\theta_{\alpha F\mathrm{p}}$. The fourth component:

$$\frac{P_{\mathrm{p}}\alpha}{2I_{zz}\pi}\tau^2\,, \tag{A10.4}$$

is the angle caused by the alpha component of $F_{\mathrm{imd}}(t)$, and can be abbreviated θ_α. The fifth component:

$$\frac{T_{\max}}{I_{zz}\pi}\tau^2\,, \tag{A10.5}$$

is the angle caused by free moment, and can be abbreviated θ_{Tz}. The last component represents the contribution of initial rotational velocity. All of these components are angles, and can be summarized as:

$$\theta_{\mathrm{r}} = \theta_{\mathrm{Fp}} + \theta_\beta + \theta_{\alpha\mathrm{Fp}} + \theta_\alpha + \theta_{\mathrm{Tz}} + \omega_0\tau\,. \tag{A11}$$

In this study, we found that humans do not precisely match deflection with body rotation, but instead begin and end turns at initial and final body angles relative to movement deflection (Fig. 1A). Separating these contributors yields a final relationship:

$$\theta_{\mathrm{d}} = \theta_{\mathrm{r}} + \theta_{\mathrm{i}} + \theta_{\mathrm{f}}\,. \tag{A12}$$

Substituting Eqn A12 into Eqn A11 and rearranging as contributions to braking, θ_β, yields:

$$-\theta_\beta = -\theta_{\mathrm{d}} + \theta_{\mathrm{Fp}} + \theta_{\alpha\mathrm{Fp}} + \theta_\alpha + \theta_{\mathrm{Tz}} + \omega_0\tau + \theta_{\mathrm{i}} + \theta_{\mathrm{f}}\,. \tag{A13}$$

Substituting $(P_{\mathrm{p}}\beta/I_{zz}\pi)\tau^2$ for θ_β and multiplying both sides by −1 results in:

$$\frac{P_{\mathrm{p}}\beta}{I_{zz}\pi}\tau^2 = \theta_{\mathrm{d}} - \theta_{\mathrm{Fp}} - \theta_{\alpha\mathrm{Fp}} - \theta_\alpha - \theta_{\mathrm{Tz}} - \omega_0\tau - \theta_i - \theta_{\mathrm{f}}\,. \tag{A14}$$

Dividing Eqn A14 by θ_{d} results in:

$$\frac{P_{\mathrm{p}}\beta}{I_{zz}\pi\theta_{\mathrm{d}}}\tau^2 = 1 - \frac{\theta_{\mathrm{Fp}} + \theta_{\alpha\mathrm{Fp}} + \theta_\alpha}{\theta_{\mathrm{d}}} - \frac{\omega_0\tau + \theta_{\mathrm{i}} + \theta_{\mathrm{f}}}{\theta_{\mathrm{d}}} - \frac{\theta_{\mathrm{Tz}}}{\theta_{\mathrm{d}}}\,. \tag{A15}$$

Substituting $\mathrm{LE}=(\theta_{\mathrm{Fp}}+\theta_\alpha+\theta_{\alpha\mathrm{Fp}})/\theta_{\mathrm{d}}$ and $\eta=(\omega_0\tau+\theta_{\mathrm{i}}+\theta_{\mathrm{f}})/\theta_{\mathrm{d}}$ into Eqn A15 allows the braking force to be predicted from:

$$F'_{\mathrm{hmax}} = \frac{\pi I_{zz}\theta_{\mathrm{d}}}{\tau^2 P_{\mathrm{p}}}\left(1 - \mathrm{LE} - \eta - \frac{\theta_{\mathrm{Tz}}}{\theta_{\mathrm{d}}}\right). \tag{A16}$$

We found free moments to be relatively small and not make a substantial contribution to running turns. Ignoring the free moment results in:

$$F'_{\mathrm{hmax}} = \frac{\pi I_{zz}\theta_{\mathrm{d}}}{\tau^2 P_{\mathrm{p}}}\left(1 - \mathrm{LE} - \eta\right), \tag{A17}$$

which is the final format of Eqn 3. It should be noted that these equations express relationships among parameters only, and could be used to predict the value of any parameter based on measured or estimated values for others. Braking forces were chosen for prediction because they: (1) are observed during turning but not during constant-average-velocity running, (2) have a large variance and (3) could potentially be modulated during a step to control body rotation. However, this does not imply that braking forces do not have other functions (such as maintaining constant velocity), or that other parameters (such as foot placement) are not actively controlled during maneuvers.

Acknowledgements

This research would not have been possible without the support of the Arizona State University (ASU) Kinesiology Program, School of Life Sciences and Graduate College. We are grateful to James Abbas and the ASU Center for Adaptive Neural Systems for use of laboratory facilities. Furthermore, we thank Carolyn Westlake for valuable input and contributions to experimental design.

Competing interests

The authors declare no competing financial interests.

Author contributions

All authors contributed to the conception, design and execution of the experiment(s). M.Q. and D.L.J. analysed the data, interpreted the results, and drafted and revised the article.

Funding

Portions of this research were supported by a Minority Access to Research Careers (National Institutes of Health) grant to the School of Life Sciences, Arizona State University. Deposited in PMC for release after 12 months.

References

Aerts, P., Van Damme, R., D'Août, K. and Van Hooydonck, B. (2003). Bipedalism in lizards: whole-body modelling reveals a possible spandrel. *Philos. Trans. R. Soc. B* **358**, 1525-1533.

Alexander, R. M. (2002). Stability and manoeuvrability of terrestrial vertebrates. *Integr. Comp. Biol.* **42**, 158-164.

Auyang, A. G., Yen, J. T. and Chang, Y. H. (2009). Neuromechanical stabilization of leg length and orientation through interjoint compensation during human hopping. *Exp. Brain Res.* **192**, 253-264.

Bencke, J., Naesborg, H., Simonsen, E. B. and Klausen, K. (2000). Motor pattern of the knee joint muscles during side-step cutting in European team handball. Influence on muscular co-ordination after an intervention study. *Scand. J. Med. Sci. Sports* **10**, 68-77.

Besier, T. F., Lloyd, D. G., Ackland, T. R. and Cochrane, J. L. (2001). Anticipatory effects on knee joint loading during running and cutting maneuvers. *Med. Sci. Sports Exerc.* **33**, 1176-1181.

Besier, T. F., Lloyd, D. G. and Ackland, T. R. (2003). Muscle activation strategies at the knee during running and cutting maneuvers. *Med. Sci. Sports Exerc.* **35**, 119-127.

Biewener, A. A. and Daley, M. A. (2007). Unsteady locomotion: integrating muscle function with whole body dynamics and neuromuscular control. *J. Exp. Biol.* **210**, 2949-2960.

Carrier, D. R., Walter, R. M. and Lee, D. V. (2001). Influence of rotational inertia on turning performance of theropod dinosaurs: clues from humans with increased rotational inertia. *J. Exp. Biol.* **204**, 3917-3926.

Chang, Y.-H., Huang, H. W. C., Hamerski, C. M. and Kram, R. (2000). The independent effects of gravity and inertia on running mechanics. *J. Exp. Biol.* **203**, 229-238.

Colby, S., Francisco, A., Yu, B., Kirkendall, D., Finch, M. and Garrett, W., Jr (2000). Electromyographic and kinematic analysis of cutting maneuvers. Implications for anterior cruciate ligament injury. *Am. J. Sports Med.* **28**, 234-240.

Cross, M. J., Gibbs, N. J. and Bryant, G. J. (1989). An analysis of the sidestep cutting manoeuvre. *Am. J. Sports Med.* **17**, 363-366.

Demes, B., Fleagle, J. G. and Jungers, W. L. (1999). Takeoff and landing forces of leaping strepsirhine primates. *J. Hum. Evol.* **37**, 279-292.

Dial, K. P., Greene, E. and Irschick, D. J. (2008). Allometry of behavior. *Trends Ecol. Evol.* **23**, 394-401.

Dickinson, M. H., Farley, C. T., Full, R. J., Koehl, M. A. R., Kram, R. and Lehman, S. (2000). How animals move: an integrative view. *Science* **288**, 100-106.

Dunbar, D. C. (1988). Aerial maneuvers of leaping lemurs – the physics of whole-body rotations while airborne. *Am. J. Primatol.* **16**, 291-303.

Eilam, D. (1994). Influence of body morphology on turning behavior in carnivores. *J. Mot. Behav.* **26**, 3-12.

Full, R. J., Kubow, T., Schmitt, J., Holmes, P. and Koditschek, D. (2002). Quantifying dynamic stability and maneuverability in legged locomotion. *Integr. Comp. Biol.* **42**, 149-157.

Glaister, B. C., Bernatz, G. C., Klute, G. K. and Orendurff, M. S. (2007). Video task analysis of turning during activities of daily living. *Gait Posture* **25**, 289-294.

Gribble, P. L., Mullin, L. I., Cothros, N. and Mattar, A. (2003). Role of cocontraction in arm movement accuracy. *J. Neurophysiol.* **89**, 2396-2405.

Hackert, R., Schilling, N. and Fischer, M. S. (2006). Mechanical self-stabilization, a working hypothesis for the study of the evolution of body proportions in terrestrial mammals? *C. R. Palevol* **5**, 541-549.

Herr, H. and Popovic, M. (2008). Angular momentum in human walking. *J. Exp. Biol.* **211**, 467-481.

Houck, J. (2003). Muscle activation patterns of selected lower extremity muscles during stepping and cutting tasks. *J. Electromyogr. Kinesiol.* **13**, 545-554.

Howland, H. C. (1974). Optimal strategies for predator avoidance: the relative importance of speed and manoeuvrability. *J. Theor. Biol.* **47**, 333-350.

Huston, R. L. and Passerello, C. E. (1982). The mechanics of human body motion. In *Human Body Dynamics: Impact, Occupation, and Athletic Aspects* (ed. D. N. Ghista), pp. 203-247. Oxford: Clarendon Press.

Jindrich, D. L. and Full, R. J. (1999). Many-legged maneuverability: dynamics of turning in hexapods. *J. Exp. Biol.* **202**, 1603-1623.

Jindrich, D. L. and Qiao, M. (2009). Maneuvers during legged locomotion. *Chaos* **19**, 026105.

Jindrich, D. L., Besier, T. F. and Lloyd, D. G. (2006). A hypothesis for the function of braking forces during running turns. *J. Biomech.* **39**, 1611-1620.

Jindrich, D. L., Smith, N. C., Jespers, K. and Wilson, A. M. (2007). Mechanics of cutting maneuvers by ostriches (*Struthio camelus*). *J. Exp. Biol.* **210**, 1378-1390.

Kane, T. R. and Scher, M. P. (1970). Human self-rotation by means of limb movements. *J. Biomech.* **3**, 39-49.

Kawamoto, R., Ishige, Y., Watarai, K. and Fukashiro, S. (2002). Influence of curve sharpness on torsional loading of the tibia in running. *J. Appl. Biomech.* **18**, 218-230.

Keppel, G. and Wickens, T. D. (eds) (2004). The two-factor within-subject design. In *Design and Analysis: a Researcher's Handbook*, Vol. 4, pp. 401-429. Upper Saddle River, NJ: Pearson Prentice Hall.

Lee, D. V., Walter, R. M., Deban, S. M. and Carrier, D. R. (2001). Influence of increased rotational inertia on the turning performance of humans. *J. Exp. Biol.* **204**, 3927-3934.

Losos, J. B. and Irschick, D. J. (1996). The effect of perch diameter on escape behaviour of *Anolis* lizards: laboratory predictions and field tests. *Anim. Behav.* **51**, 593-602.

McGowan, C. P., Baudinette, R. V., Usherwood, J. R. and Biewener, A. A. (2005). The mechanics of jumping versus steady hopping in yellow-footed rock wallabies. *J. Exp. Biol.* **208**, 2741-2751.

McLean, S. G., Huang, X. M., Su, A. and Van Den Bogert, A. J. (2004). Sagittal plane biomechanics cannot injure the ACL during sidestep cutting. *Clin. Biomech. (Bristol, Avon)* **19**, 828-838.

Orendurff, M. S., Segal, A. D., Berge, J. S., Flick, K. C., Spanier, D. and Klute, G. K. (2006). The kinematics and kinetics of turning: limb asymmetries associated with walking a circular path. *Gait Posture* **23**, 106-111.

Patla, A. E., Adkin, A. and Ballard, T. (1999). Online steering: coordination and control of body center of mass, head and body reorientation. *Exp. Brain Res.* **129**, 629-634.

Qiao, M. and Jindrich, D. L. (2012). Task-level strategies for human sagittal-plane running maneuvers are consistent with robotic control policies. *PLoS ONE* **7**, e51888.

Rand, M. K. and Ohtsuki, T. (2000). EMG analysis of lower limb muscles in humans during quick change in running directions. *Gait Posture* **12**, 169-183.

Scholz, J. P. and Schöner, G. (1999). The uncontrolled manifold concept: identifying control variables for a functional task. *Exp. Brain Res.* **126**, 289-306.

Stacoff, A., Steger, J., Stüssi, E. and Reinschmidt, C. (1996). Lateral stability in sideward cutting movements. *Med. Sci. Sports Exerc.* **28**, 350-358.

Taylor, M. J. D., Dabnichki, P. and Strike, S. C. (2005). A three-dimensional biomechanical comparison between turning strategies during the stance phase of walking. *Hum. Mov. Sci.* **24**, 558-573.

Van Damme, R., van Dooren, T. J. M.; Van damme R; Van dooren TJ (1999). Absolute versus per unit body length speed of prey as an estimator of vulnerability to predation. *Anim. Behav.* **57**, 347-352.

Walter, R. M. (2003). Kinematics of 90 degrees running turns in wild mice. *J. Exp. Biol.* **206**, 1739-1749.

Yen, J. T. and Chang, Y. H. (2010). Rate-dependent control strategies stabilize limb forces during human locomotion. *J. R. Soc. Interface* **7**, 801-810.